PharmacologyOnLine
April 30, 2013
Archives • 2013 • vol.1 • 206 - 217

Mass spectra analysis of *H. sabdariffa* L anthocyanidins and their *in silico* corticosteroid-binding globulin interactions

Omotuyi[1,3,*], I.O.; Elekofehinti[2,3], O.O.; Ejelonu[3] O.C.; Obi[4], F.O
[1]Department of Molecular Pharmacology and Neuroscience, Nagasaki University, Japan
[2]Biochemical Toxicology Unit, Universidade Federal de Santa Maria Rs, Brazil
[3]Adekunle Ajasin University, Akungba-Akoko. Nigeria
[4]Department of Biochemistry, University of Benin, Edo State, Nigeria
*Omotuyi, I.Olaposi
Department of Molecular Pharmacology and Neuroscience, Nagasaki University, Japan
email: bbis11r104@cc.nagasaki-u.ac.jp

Summary

Anthocyanins, structurally characterized as water soluble glycosides of polyhydroxyl and polymethoxyl derivatives of 2-phenyl bezopyryliium confer redness to the cloves of *H. sabdariffa* Lin. Using Mass spectrophotomery, pelargodin (m/z 271.23), cyanidin (m/z 287), Peonidin (m/z 299.28), delphinidin (m/z 301), petunidin (m/z 317.31) and acetylated malvidin (m/z 391.33) have been identified as the major anthocyanidins in *H. sabdariffa* hydrolysate. The structures of the anthocyanidins and their C-3 glycosides have been docked into the cortisol-binding pocket of corticosteroid binding globulin (CBG). Our data strongly indicate that the contribution of pi-electron between the heterocyclic bezopyrylium rings of anthocyanidins and the indole ring of tryptophan 352 play a key role in stabilizing the complex. The GBVIWSA free energy of interaction predict that cortisol is a better ligand for CBG transportation with (-8.2618kcal/mol) while the lowest value recorded for anthocyanin/anthocyanidins is -6.5539kcal/mol (delphinidin-3-glucoside). Our data therefore suggest that cortisol transportation may only be altered in situation where plasma anthocyanins/anthocyanidins are in excess of cortisol.

Keywords: Hibiscus sabdariffa L. Anthocyanins, Anthocyanidins, cortisol, CBG, GBVIWSA free energy

Introduction

Anthocyanin pigment confers brilliant coloration on many fruits and vegetables. Their nutraceutical values have been a subject of intense study with strong data in support of antioxidant [1], anti-cancer [2,3], and anti-inflammatory potencies [4]. These properties and very high LD50 value (>2000mg/kg) [5] (Pourrant et al., 1967) of anthocyanins have influenced their use as safe food additives [6]. Previously, we have reported altered circulating levels of reproductive hormone in rabbits [7] during oral anthocyanin treatment and in the article, we have suggested a possible reprodictive toxicity.

Now we have employed mass spectrophometry method to identify the major anthocyanidins in *H. sabdariffa L.* and in silico methods (Molecular Operating Environment) to estimate its binding affinity for corticosteroid binding globulin (CBG) as the first step in exploring its role during stress and its anti-obesity potencies.

CBG also known as transcortin is SERPINA6-encoded plasma protein of liver origin [8], which is directly involved in the regulation of the bioavailability and metabolic clearance of cortisol, progesterone, aldosterone and 11-deoxycorticosterone [9,10]. Plasma CBG-cortisol is a reserviour of biologically inactive cortisol, in free state. The diffusion-mediated cellular uptake of cortisol is associated with cellular stress response, gluconeogenesis, antiinflammation, lipid and protein metabolism [11,12].

Chemical, phytochemical or pharmaceutical agent that shifts the equilibrium of cortisol-CBG interaction towards dissociation will increase its urinary excretion and may alter the concentration of biologically active cortisol available for diffusion into target tissues [13]. Increased urinary excretion of unmetabolized cortisol via flavonoid-mediated 11beta-hydroxysteroid dehydrogenase inhibition has been reported [14] and the gains in terms of antiobesity and altered lipid metabolism have also been documented [15]. However, the implication of continuous consumption of phytochemical agents on the HPA axis remains largely unclear.

Here, we explore the influence of anthocyanin on cortisol transportation in the blood based on computational docking simulations and free energy calculations.

In our model, intact anthocyanin of hibiscus sabdariffa exhibit slightly lower affinity for CBG than cortisol and are predicted to alter CBG-cortisol binding only in situations of excessive consumption and rapid absorption which allows a significantly higher blood concentration of anthocyanins/anthocyanidins in far excess of cortisol.

Materials and methods

Anthocyanin extraction and partial purification and hydrolysis protocols

The acid-extracted (0.01% HCL) extract of H. sabdariffa clove was purified on C-18 sep-pak cartridge (Waters Associates, Milford MA). HCL (0.01%) was used for elution of non-covalently bound sugars, organic acids and other water soluble compounds. Anthocyanins were eluted with HCL acidified methanol (0.01 % v/v HCL) [16]. The sample was directly hydrolyzed with 2N HCL at 80°C for 30min to give the full complement of anthocyanidins and their acylated groups.

Mass Spectroscopic analysis of Anthocyanins

The hydrolyzed anthocyanin was diluted in methanol and analyzed on JOEL AccuTOF™ mass spectrophotometer system which consists of standard Electrospray Ion Source (ESI) and a JOEL MassCenter™ workstation. The ESI source was turned to positive mode. The needle and MCP voltage were set at 2000 and 2600V respectively.

The orifice chamber temperature was 80°C while the voltages were switched between 35 and 120V. The desolvation chamber temperature was set at 250°C. The structures of the anthocyanin compounds were retrieved from pubchem database (www.pubchem.ncbi.nlm.gov) based on their molecular weights. Retrieved structures were used

for docking studies.

In Silico Docking and Scoring Analyses on MOE platform

Flexible ligand-docking was performed using MOE (molecular operating environment, 2011.10) platform [17]. The 3D structure of corticosteroid binding globulin (CBG) used was retrieved from Protein Data Bank (PBD ID-2V95) (www.pdb.org) [18]. The structure was uploaded into the MOE software, water molecules and other non-amino acid component including were removed, 3D protonation and parametization were done using the protein preparation pull-down menu, all the missing atoms, incorrect bond stretch and length were corrected. The LigX menu was used to tether heavy atoms and recheck the parameters before docking. The docking simulation was done using the following protocols: Poses were generated using triangle matcher placement. Receptor + solvent mode was assigned to the receptor while the ligand (site) was defaulted to bind on selected residues which were recognized as Hydrocortisol binding residues from the 3D structure. The first scoring was done using London dG defined by the equation below:

$$\Delta G = c + E_{flex} + \sum_{h-bonds} c_{HB} f_{HB} + \sum_{m-lig} c_M f_M + \sum_{atoms\ i} \Delta D_i$$

$$\Delta D_i = c_i R_i^3 \left\{ \iiint_{u \notin A \cup B} |u|^{-6}\, du - \iiint_{u \notin B} |u|^{-6}\, du \right\}$$

D_i is the desolvation energy, c represents the average gain/loss of rotational and translational entropy E_{flex} is the energy due to loss of flexibility of the ligand. F_{HB} measures geometric imperfections of hydrogen bonds. C_{HB} is the energy of an ideal hydrogen bond, Fm measures geometric imperfections of metal ligation while Cm is the energy of an ideal metal ligation. A and B are protein and/or ligand volumes with atoms *i belonging to volume B; R_i is the solvation radius of atom i. C_i is the desolavation coefficient of atom i.*

Each pose was refined by forcefield and subsequently rescored using the GBVI/WSA dG function as defined below:

$$\Delta G \approx c + \alpha \left[\frac{2}{3}(\Delta E_{coul} + \Delta E_{sol}) + \Delta E_{vdw} + \beta \Delta SA_{weighted} \right]$$

C represents the average gain/loss of rotational and translational entropy, á is forcefield-dependent constant, E_{coul} is the columbic electrostatic term, E sol is the solvation electrostatic term, E_{vdw} is the van der Waals contribution to binding and $SA_{weighted}$ is the surface area weighted by exposure. The veracity of GBVI/WSA dG as scoring function has been validated by [19]. The 2D depiction of the protein-ligand complex has been reported by [20].

PYMOL (Delano Scientific LLC, USA) was used for surface map visualization for ligand and receptor interaction.

see Fig. 1.0

see Fig. 2.0a

see Fig. 2.0b

see Fig. 3.0a

see Fig. 3.0b

see Fig. 3.0c

see Fig. 3.0d

see Fig. 3.0e

see Fig. 3.0f

Results

Hibiscus sabdariffa L. is rich in diversely acylated and glycosylated Anthocyanidins

The presence of anthocyanins in *H. sabdariffa* calyx has been reported in *H. sabdariffa* [21,22,23], most of the ethnobotanical use and biological activities of *H. sabdariffa* extract have been attributed to their anthocyanin content [24,25]. There is growing number of publications on the bioactivity of anthocyanin extract of *H. sabdariffa* due to

increased research effort aimed at documenting information on the individual anthocyanins. Fig 1.0 shows the mass spectrum of *H. sabdariffa* hydrolysate.

We have identified five classes of anthocyanidin including pelargodin (m/z 271.23), cyanidin (m/z 287), Peonidin (m/z 299.28), delphinidin (m/z 301), petunidin (m/z 317.31) and acetylated malvidin (m/z 391.33). The presence of delphinidin, cyanidin, petunidin and Peonidin glycosides in the cloves *of H. sabdariffa* based on HPLC analysis. The figure also shows many background peaks at (M/Z) less than 200; this data partially indicate an impure effluent at the C-18 stage of purification but a critical appraisal of the data reveals the presence of unique peaks above 100 level of abundance (blue dotted line). Peaks 111.06 and 119.05 are most probably succinic acid in non-hydrated and hydrated forms respectively, peak 206 and peak 223 are likely sinapic acid and its hydrated form respectively. Peak 169 may be dehydrated ferulic acid, p-coumaric acid or a rhamnose molecule. Peak 148.99 is most likely a pentose while peak 177.03 is predicted to be hexose molecules.

Acidic groups predicted here have been reported in diverse anthocyanin and they dictate the acylation pattern and colour stability of their anthocyanidin core [27]. The difference in acylation patterns of tradescantia (*Tradescantia pallida*, v.), concord grapes and red cabbage anthocyanin accounts for the difference in their colour stability in solution of different pH [28]. Anthocyanins colour stability is positively correlated with increased acylation [29].

Furthermore, anthocyanins with aromatic acylation result in higher stability than aliphatic acylated anthocyanin [30] as observed in Caffeic acid and *p*-coumaric acid [31] conjugated anthocyanins. Glucose and galactose and rhamnose are the major hexose conjugated to anthocyanidins while pentoses such as rhamnose, arabinose and xylose have also been reported [32]. Other higher order sugars found in anthocyanins are rutinose, sophorose, sambubiose and glucorutinose [33].

In silico analysis *shows H. sabdariffa* anthocyanidins bind into similar pocket as Hydrocortisol in CBG

Corticosteroid-binding globulin (CBG) belongs to serine proteinase inhibitor (serpin) family. It transports glucocorticoids and some other steroids in the blood [9,10]. The steroid-binding residues of CBG are R10, A13, P14, V17, Q224, D226, T232, R252, I255, G259, K260, F357, K359, and W362 [18]. To verify the residues involved in cortisol binding in silico, the 3D crystal structure of CBG obtained from Protein Data Bank (2V95) was prepared for docking by removal of the water molecules and the cortisol ligand. MMFF94x potential set up was used to minimize cortisol in accordance with parametization of small organic molecules in gas phase. This molecule was redocked into the pocket using the protocol previously explained in the materials and method section. The GBVIWSA free energy obtained during this step was -5.8kcal/mol (data not shown) and we plotted the 2D interaction to confirm the residues. We found that the residues were quite different from the ones reported earlier [35]. We repeated the protein preparation step but this time, preserving the 4 water molecules located in the active site of the original PDB file. -8.2618kcal/mol free energy obtained using this new protocol and all the residues identified by [35] and colleagues were confirmed. The 3D space presented as helix and sheet structure (fig 2.0bi) shows that cortisol binds into a triangle-like space contributed by residues in sheet-B2-5 (Q224. D226, T232, F357, K359, W362), helix-H (I225, R252, K260, G259) and Helix-A (A13, P14 and V17) fig (2.0bii). Anthocyanins and anthocyanidins identified in *H. sabdariffa* cloves using mass spectroscopy were retrieved from pubchem database or drawn using the builder menu of MOE software (fig 2.0a).

Although, all the predicted structures were docked to obtain their free energies of binding, pelargonidin, cyanidin, Peonidin and malvidin adjudged to be more abundant according to the spectra data were shown (fig 3.0a-f). Testosterone and estradiol were used as positive control due to its more structural similarity to cortisol than antho-

cyanins and anthocyanidins, this step attempts to evaluate CBG specificity for cortisol.

The 2D depiction of ligand-CBG interactions for all the structures investigated are shown in figures 3.0a-f. Hydrophobic patch, pi-electron interaction and hydrogen bonding are the major forces involved in the interaction between CBG and cortisol (fig 3.0ai). Cortisol ring-A atoms (C_{1-3}) are proximal to A13, P14 and V17 residues of CBG (helix-A, fig 2.0b) therefore may interact via hydrophobic interaction. Pi-electron system is contributed by indole ring of Trp362 (sheet-B) and the aromatic B-ring of cortisol. Hydrogen bonding interaction is predicted between amido nitrogen of Gln224 and C-21 carbonyl oxygen of cortisol; a water molecule and Gly259 contribute to the stability of the hydrogen bond. Asp256 (helix-H) and a water molecule interact with C-11 hydroxyl group. The surface and map is shown in fig 3.0aii. Testosterone interaction at the cortisol-binding domain is predicated upon hydrophobic interaction between Phe367 and the A-ring, Ile255 and D-ring, pi-electron system between indole group of Trp362 and bridge hydrogen between rings B and C. A hydrogen bonding interaction is predicted between guanidino group of Arg252 and the C-17 hydroxyl group of testosterone (fig 3.0bi). The surface and map is shown in fig 3.0bii. Interaction between cortisol-binding residues of CBG and pelargonidin is predicated upon hydrophobic patch contributed by Ala13, Ile255, Phe357, Val17, Pro14 and Phe234, pi-electron system between indole group of Trp362 and Benzopyran-3-ol (fused rings A and B) of pelargonidin (fig 3.0ci) surface and map depiction is shown in fig 3.0cii. 2D interaction between cyanidin and cortisol-binding pocket of CBG is depicted in figure (3.0di). Arg252, Gln224, Lys359 and Thr232 contribute to stability of the complex via interaction with C-5, C-3, and C-5^1 hydroxyl groups of cyanidin. Trp352 interacts with pyran-3ol ring via pi-electron system. Ala13, Pro14 and Val17 may contribute to hydrophobic interaction due to their proximities to ring-A. Surface and map depiction for this interaction is shown in fig 3.0dii. The interaction between peonidin and cortisol-binding pocket of CBG is principally dictated by hydrophobic interaction between Ala13 and Val17 proximal to the 6,8-dihydroxyl benzopyran-3-ol group, hydrogen-bonding interaction between Gln224, Gly259 and C-4^1 hydroxyl group (ring C) which is further stabilized by a water molecule. Pi-electron system is also predicted between Phe357 and the C-3 hydroxyl group of the pyran moiety, and between Trp352 and fused 3, 6,8-trihydroxylbenzopyranol-group (fused A and B ring, fig 3.0ei) . The detailed surface and map depiction for this interaction is shown in fig 3.0eii. Malvidin which we have predicted as the most abundant based on the spectra data shows similar binding pattern. Lys359, Thr232, Gly259 and Gln224 constitute an hydrophilic environment proximal to C-3^1, C-5^1 dimethyoxy-phenyl group (ring C), Ala13 and Phe234 also contribute hydrophobic interaction with fused rings A and B. Trp363 and 5,7-dihydroxyl-benzopyran-3-ol interact via pi-electron system. Asp256 and one water molecule interact with C-3 hydroxyl group of ring-B via hydrogen bond (fig 3.0f1). The detailed surface and map depiction for this interaction is shown in fig 3.0fii.

Free energy estimation predicts weak interaction between CBG and H. sabdariffa anthocyanins

GBVIWAS free energy of binding represents the contribution of rotational and translational entropy, forcefield-dependent columbic electrostatic van der Waals interaction, solvation electrostatic interaction, and surface area weighted by exposure to the recognition and binding of a ligand to the pocket of a receptor and this method of free energy estimation has been sown to correlate strongly to experimental values [18]. We therefore used GBVIWSA method to estimate the free energy of binding of the natural ligand (cortisol), natural ligand structural mimics (estradiol and testosterone), and anthocyanidins and their glycone derivatives with the aim of gaining insight into possible competitive inhibition of cortisol-binding under physiological conditions. Table 1.0 shows that cortisol has the lowest free energy (<-8.0kcal/mol) while the highest free energy was estimated for testosterone (-3.0513kcal/mol). These values are strong indications

that testosterone may not be transported by CBG thereby authenticating the role of SHBG rather than CBG as transporter of choice for testosterone as previously reported [34]. Delphinidin-3-glucoside, estradiol, delphinidin, pelargonidin, malvidin-3-glucoside and peonidin has comparatively similar binding free energies (between -6.0098 to -6.5539kcal/mol).

Although, the free energies here are significantly lower than those recorded for cortisol, significantly higher blood concentration of delphinidin-3-glucoside, delphinidin, pelargonidin, malvidin-3-glucoside and peonidin in excess of cortisol may change the equilibrium towards anthocyanin binding in accordance with mathematical relationship between free energy of binding and dissociation constant, and between equilibrium constant and concentration [35]. This information is particularly important because plasma cortisol concentration range between approximately 15ug/dL under resting conditions and approximately 160ug/dL under stress conditions in humans [36,37] while blood concentration of anthocyanin after consumption may reach approximately 2.0mg/dL after 1 hr of ingestion and only decrease by 50% after 4 hr [40,41,42]. Statistically, anthocyanins may effect transportation of cortisol under basal conditions. Pelargonidin-3-glucoside, petunidin, petunidin-3-glucoside, cyanidin, peonidin-3-glucoside, malvidin and cyanidin-3-glucoside have lower binding affinities for CBG compared to the delphinidin-3-glucoside, delphinidin, pelargonidin, malvidin-3-glucoside and peonidin.

Discussion

While we are presently working on non-acid based extraction protocol for H. sabdariffa anthocyanins with the aim of preserving the glycone portions, perfection of this protocol will enable us characterize individual anthocyanins using HPLC, MS and NMR (proton and carbon) without need for hydrolysis. Here, we have identified the major anthocyanidins as pelargodin, cyanidin, Peonidin, delphinidin, petunidin and acetylated malvidin based on mass spectroscopy analysis. This data agree with HPLC chromatogram reported by [26]. Succinic acid, sinapic acid, ferulic acid, p-coumaric acid, a rhamnose, pentose and hexose molecules have also been identified as molecular basis for the formation of anthocyanins and various acylated analogues of anthocyanins. Acylation is reportedly important in colour and stability of anthocyanin [29,30] glycosylation essentially facilitates their transportation into the plant vacuole. In animals, rapid absorption of anthocyanin after ingestion has been reported [38,30,40] but has not well correlated with tissue distribution, this information makes the activity of anthocyanins in the blood a very important study question.

Many biological roles of anthocyanins are already documented and the list is growing [1,2,3,4] here we focused on its effect on cortisol metabolism by exploring potential modulatory role in cortisol transportation through CBG mechanisms. The focus on cortisol is predicated on its importance to stress response, glucose metabolism [41] inflammatory response [42] and adipokinesis [43,44]. In a related report, consumption of grapefruit juice, rich in naringenin, quercetin and hesperetin, have been shown to modulate cortisol metabolism and excretion [14]. Other authors have reported 11beta Hydroxyl-steroid dehydrogenase inhibition [45] by flavonone**.** This enzyme catalyses the interconversion of cortisol (active) to cortisone (inactive) via oxido-reduction mechanisms. Some authors have submitted that an indirect 11beta Hydroxyl-steroid dehydrogenase inhibition may also occur through NADPH depletion mechanisms profoundly via inhibition of glucose-6-phophate translocase which limits microsomal glucose-6-phosphate concentration [46,47,48] and NADPH generation. It will be necessary to mention here that since microsomal glucose-6-phosphatase is directly involved in blood glucose buffering and gluconeogenesis, the role of anthocyanin as antiobesity and anti-gluconeogenic agent become easier to comprehend [49]. Other aspects of cortisol function reportedly inhbited by anthocyanin include glucocorticoid-receptor translocation and glucocorticoid-induced expression of

PEP-CK [50].

Here, we have discovered for the first time that anthocyanidins and their glycone derivatives can bind cortisol-binding pocket of CBG but however with lower affinity compared to cortisol its natural ligand. The interaction between CBG and anthocyanins/anthocyanidins are essentially stabilized by pi-electron system involving the benzopyranol rings of anthocyanin/anthocyanidin and the heterocyclic indole ring of Trp352, contributions of hydrogen bonding and hydrophobic interaction were also highlighted in the result section. Delphinidin-3-glucoside, delphinidin, pelargonidin, malvidin-3-glucoside and peonidin have comparatively similar binding free energies of binding with approximately 2kcal/mol energy higher than the value recorded for cortisol. The mathematical relationship that exist between free energy of binding and dissociation constant, and between equilibrium constant and concentration [37] allows the equilibrium to shift towards anthocyanin/anthocyanidin binding in situation where their concentration is in excess of cortisol, this is particularly true for basal cortisol transportation as approximately 15ug/dL cortisol is found in the blood under resting conditions [38] while blood concentration of anthocyanin after consumption may reach approximately 2.0mg/dL after ingestion [40,41,42]. The metabolic implication of this data is increased urinary excretion of cortisol, reduced gluconeogensis and lipodystrophy.

Conclusion

Based on *in silico* free energy estimation, specific and high affinity interaction has been established between naturally occuring *H. sabdariffa* anthocyanins and anthocyanidins and cortisol-binding Pocket of CBG. Given the relationship that exist between free energy and dissociation constant, we predict a possible displacement of cortisol from binding pocket on CBG under excess anthocyanin/anthocyanidin concentration above cortisol levels. This data therefore provides another insight into the mechanism of functional and metabolic antagonism that exist between anthocyanins and cortisol.

References

1. Zhang Y, Seeram NP, Lee R, Feng L, Heber D. Isolation and identification of strawberry phenolics with antioxidant and human cancer cell antiproliferative properties. J Agric Food Chem 2008; 56: 670-675.
2. Chen PN, Kuo WH, Chiang CL, et al. Black rice anthocyanins inhibit cancer cells invasion via repressions of MMPs and u-PA expression. Chem Biol Interact 2006; 163: 218-229.
3. Gerhauser, C. Cancer chemopreventive potential of apples, apple juice, and apple components. Planta Med 2008; 74: 1608-1624.
4. Hou DX, Masuzaki S, Hashimoto F, et al. Green tea proanthocyanidins inhibit cyclooxygenase-2 expression in LPS activated mouse macrophages: molecular mechanisms and structure activity relationship. Arch Biochem Biophys 2007; 460: 67-74.
5. Pourrat H, Bastide P, Dorier P, Tronche P. Préparation et activité thérapeutique de quelques glycosides d'anthocyanes. Chim Thérap 1967; 2: 33-38.
6. Strack D, Wray V. The anthocyanins In The Flavonoids: Advances in Research Since 1986 (J.B. Harborne, ed.) Chapman and Hall. 1994.
7. Omotuyi IO, Ologundudu A, Onwubiko VO, Wogu MD, Obi FO. Hibiscus sabdariffa Linn anthocyanins alter circulating reproductive hormones in rabbits (Oryctolagus cuniculus). J Diabetes Endocrinol 2010; 1: 36-45.
8. Hammond GL, Smith CL, Goping IS, et al. "Primary structure of human corticosteroid binding globulin, deduced from hepatic and pulmonary cDNAs, exhibits homology with serine protease inhibitors". Proc Natl Acad Sci 1987; 84: 5153-5157.
9. Dixon PF. The kinetics of the exchange between transcortin-bound and unbound cortisol in plasma. J Endocrinol 1968; 40: 457-465.
10. Breuner CW, Orchinik M. Plasma binding proteins as mediators of corticosteroid action in vertebrates. J Endocrinol 2002; 175: 99-112.
11. Elenkov IJ, Webster EL, Torpy DJ, Chrousos GP. Stress, corticotropin-releasing hormone, glucocorticoids, and the immune/inflammatory response: acute and chronic effects. Ann NY Acad Sci 1999; 876: 1-11.
12. Tsigos C, Chrousos GP. Hypothalamic-pituitaryadrenal axis, neuroendocrine factors and stress. J. Psychosom. Res 2002; 53: 865-871.
13. Mendel CM. The free hormone hypothesis: a physiologically based mathematical model. Endocr. Rev 1989; 10: 232-274.
14. Lee YS, Lorenzo BJ, Koufis T, Reidenberg MM. Grapefruit and its flavonoids inhibit 11beta-hydroxysteroid dehydrogenase. Clin Pharmacol 1996; 59: 62-71.
15. Khani S, Tayek JA. Cortisol increases gluconeogenesis in humans: its role in the metabolic syndrome. Clin Sci 2001; 101: 739-747.
16. Pushpa S, Murthy MR, Manjunatha G, Sulochannama M, Madhava N. Extraction, Characterization and Bioactivity of Coffee Anthocyanins. Eur J Bio Sci 2012; 4: 13-19.
17. Molecular Operating Environment (MOE), 2011.10; Chemical Computing Group Inc., 1010 Sherbooke St. West, Suite #910, Montreal, QC, Canada, H3A 2R7.
18. Klieber MA, Underhill C, Hammond GL, Muller YA. Corticosteroid-binding Globulin: Structural Basic for Steroid transport and Proteinase-triggered release. J Biol Chem 2007; 282: 29594-29603.

19. Corbeil CR, Williams CI, Labute P. Variability in docking success rates due to dataset preparation. J Comput Aided Mol Des. 2012; (DOI: 10.1007/s10822-012-9570-1).
20. Clark AM, Labute P. Depiction of protein-Ligand Complexes. J Chem Inf Model 2007; 47: 1933-1944.
21. Du CT, Francis FJ. Anthocyanins of roselle (Hibiscus sabdariffa L.). J Food Sci 1973; 38: 818.
22. Tsai PJ, McIntosh J, Pearce P, Camden B, Jordan BR. Anthocyanin and antioxidant capacity in roselle (Hibiscus sabdariffa L.) extract. Food Res Int 2002; 35: 351-356.
23. Tsai PJ, Huang HP. Effect of polymerization on the antioxidant capacity of anthocyanins in roselle. Food Res Int 2004; 37: 313-318.
24. Franworth NR, Bunyapraphatsara N. Thai medicinal plants. Pracha-chon Press, Bangkok. 1992; 163-166.
25. Hirunpanich V, Utaipa A, Morales NP, et al. Hypocholesterolemic and antioxidant effects of aqueous extracts from the dried calyx of Hibiscus sabdariffa L. in hypercholesterolemic rats. J EthnoPharmacol 2006; 103: 252-260.
26. Ologundudu AO, Ologundudu OM, Oluba IO, Omotuyi IO, Obi FO. Effect of Hibiscus sabdariffa anthocyanins on 2, 4-dinitrophenylhydrazine-induced tissue damage in Rabbits. J. Toxicol Environm Health Sci 2010; 2: 1-6.
27. Bassa IA, Francis FJ. Stability of anthocyanins from sweet potatoes in a model beverage. J. Food Sci. 1987; 52: 1753-1754.
28. Baublis A, Spomer A, Berber-Jimenez MD. Anthocyanin pigments: comparison of extract stability. J Food Sci 1994; 59: 1219-1233.
29. Rodriguez-Saona LE, Giusti MM, Wrolstad RE. Color and pigment stability of red radish and red-fleshed potato anthocyanins in juice model systems. J Food Sci 1999; 64: 451-456.
30. Stintzing FC, Carle R. Functional properties of anthocyanins and betalains in plants, food, and in human nutrition. Trends Food Sci Technol 2004; 15: 19-38.
31. Giusti MM, Rodriguez-Saona LE, Wrolstad RE. Molar absorptivity and color characteristics of acylated and non-acylated pelargonidin-based anthocyanins. J Agric Food Chem 1999; 47: 4631-4637.
32. De Ancos B, Gonzalez E, Cano MP. Differentiation of raspberry varieties according to anthocyanin composition. Food Res Tech 1999; 208: 33-38.
33. Kähkönen MP, Heinämäki J, Ollilainen V, Heinonen M. Berry anthocyanins: Isolation, identification and antioxidant activities. J Sci Food Agric 2003; 83: 1403-1411.
34. Hammond GL, Bocchinfuso WP. Sex hormone-binding globulin: gene organization and structure/function analyses. Horm Res 1996; 45: 197–201.
35. Srebrenka R. Mathematics, Thermodynamics, and Modeling to Address Ten Common Misconceptions about Protein Structure, Folding, and Stability. CBE Life Sci Educ 2010; 9: 189-195.
36. Meyerhoff JL, Oleshanshy MA, Mougey EH. Psychological stress increases plasma levels of prolactin, cortisol, and POMC-derived peptides in man. Psychosom Med 1988; 50: 295-303.
37. Esteban NV, Loughlin T, Yergey AL, et al. Daily cortisol production rate in man determined by stable isotope dilution/mass spectrometry. J Clin Endocrinol Metab 1991; 72: 39-45.
38. Cao G, Muccitelli HU, Sanchez-Moreno C, Prior RL. Anthocyanins are absorbed in glycated forms in elderly women: a pharmacokinetic study. Am J Clin Nutr 2001; 73: 920-926.
39. Wu X, Cao G, Prior RL. Absorption and metabolism of anthocyanins in elderly women after consumption of elderberry or blueberry. J Nutr 2002; 132: 1865-1871.
40. Talavéra S, Felgines C, Texier O, et al. Anthocyanins are efficiently absorbed from the stomach in anesthetized rats. J Nutr 2003; 133: 4178-4182.
41. Christiansen JJ, Djurhuus CB, Gravholt CH, et al. Effects of cortisol on carbohydrate, lipid, and protein metabolism: studies of acute cortisol withdrawal in adrenocortical failure. J Clin Endocrinol Metab 2007; 92: 3553-3559.
42. DeRijk R, Michelson D, Karp B, et al. Exercise and circadian rhythm-induced variations in plasma cortisol differentially regulate interleukin-1 beta (IL-1 beta), IL-6, and tumor necrosis factor-alpha (TNF alpha) production in humans: high sensitivity of TNF alpha and resistance of IL-6. J Clin Endocrinol Metab 1997; 82: 2182-2191.
43. Gavrila A, Peng CK, Chan JL, et al. Diurnal and ultradian dynamics of serum adiponectin in healthy men: comparison with leptin, circulating soluble leptin receptor, and cortisol patterns. J Clin Endocrinol Metab 2003; 88: 2838-2843.
44. Fallo F, Scarda A, Sonino N, Paoletta A, et al. Effect of glucocorticoids on adiponectin: a study in healthy subjects and in Cushing's syndrome. Eur J Endocrinol 2004; 150: 339-344.
45. Schweizer RA, Atanasov AG, Frey BM, Odermatt A. A rapid screening assay for inhibitors of 11beta-hydroxysteroid dehydrogenases (11beta-HSD): flavanone selectively inhibits 11beta-HSD1 reductase activity. Mol Cell Endocrinol 2003; 30: 212: 41-49.
46. Parker JC, VanVolkenburg MA, Levy CB, et al. Plasma glucose levels are reduced in rats and mice treated with an inhibitor of glucose-6-phosphate translocase. Diabetes 1998; 47: 1630-1636.
47. Arion WJ, Canfield WK, Ramos FC, et al. Chlorogenic acid and hydroxynitrobenzaldehyde: New inhibitors of hepatic glucose-6-phophatase. Arch. Biochem Biophys 1997; 339: 315-322.
48. Arion WJ, Canfield WK, Ramos FC, et al. Chlorogenic acid analogue S 3483: a potent competitive inhibitor of the hepatic and renal glucose-6-phosphatase systems. Arch Biochem Biophys 1998; 351: 279-285.
49. Oluyemi KA, Omotuyi IO, Jimoh OR, et al. Erythropoietic and anti-obesity effects of Garcinia cambogia (bitter kola) in Wistar rats. Biotechnol Appl Biochem 2007; 46: 69-72.
50. Atanasov AG, Dzyakanchuk AA, Schweizer RA, et al. Coffee inhibits the reactivation of glucocorticoids by 11betahydroxysteroid dehydrogenase type 1: a glucocorticoid connection in the antidiabetic action of coffee. FEBS Lett 2006; 580: 4081-4085.

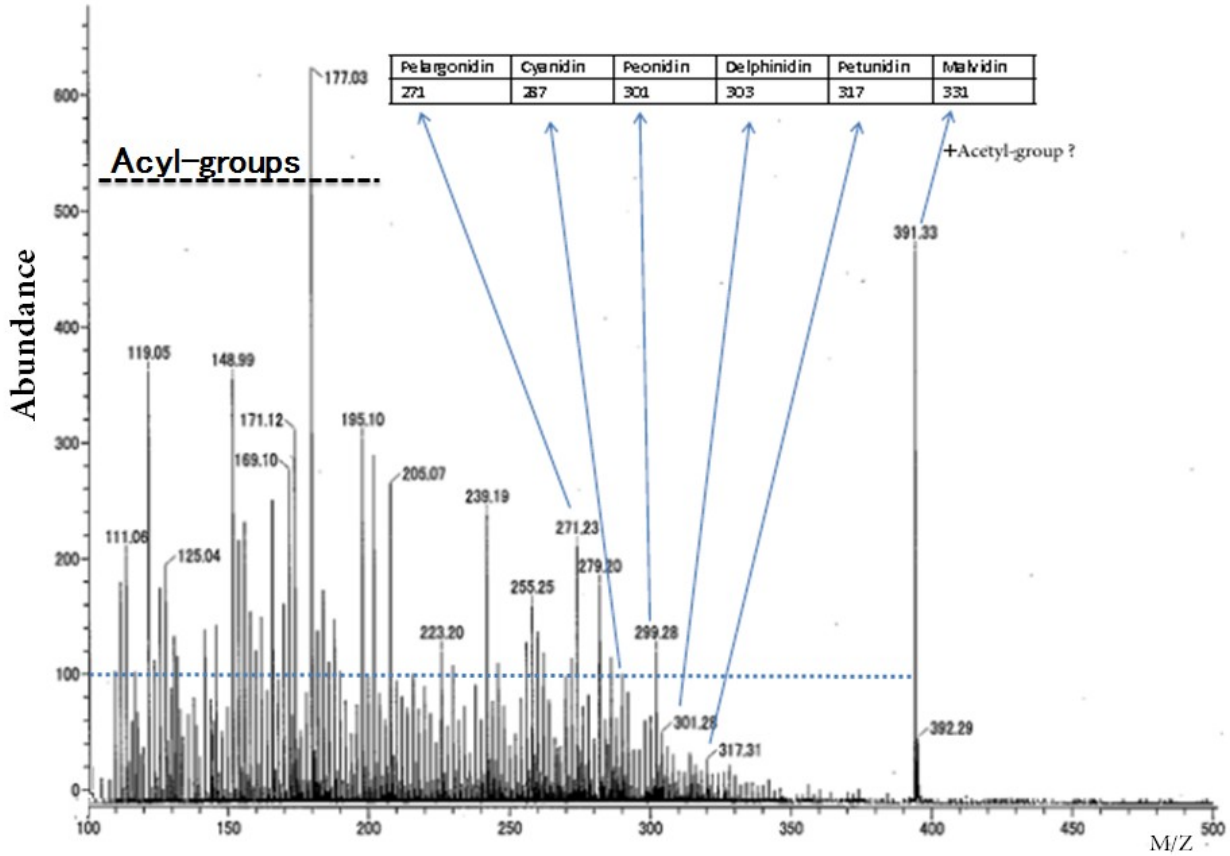

Figure 1.0. Mass Spectra of *H. Sabdariffa* Anthocyanidins and low molecular weight acyl, and sugar-related groups.

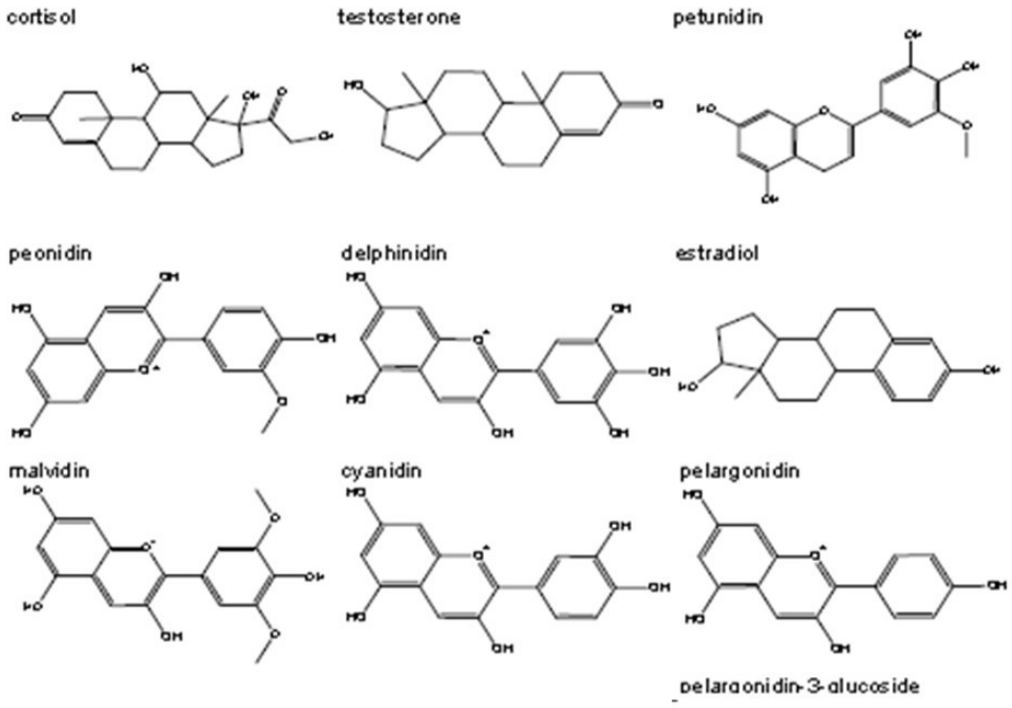

Figure 2.0a. Structures of *H. Sabdariffa* Anthocyanidins, cortisol and testosterone. Anthocyanins used for docking are designated as "C-3" glycosylated anthocyanidins.

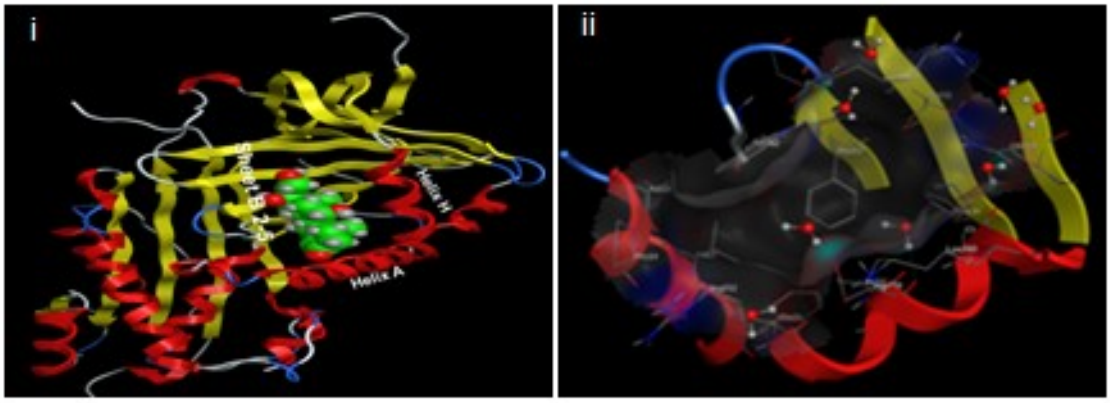

Figure 2.0b. Cortisol-binding pocket of CBG i) helics and sheets depiction, ii) surface and map depiction.

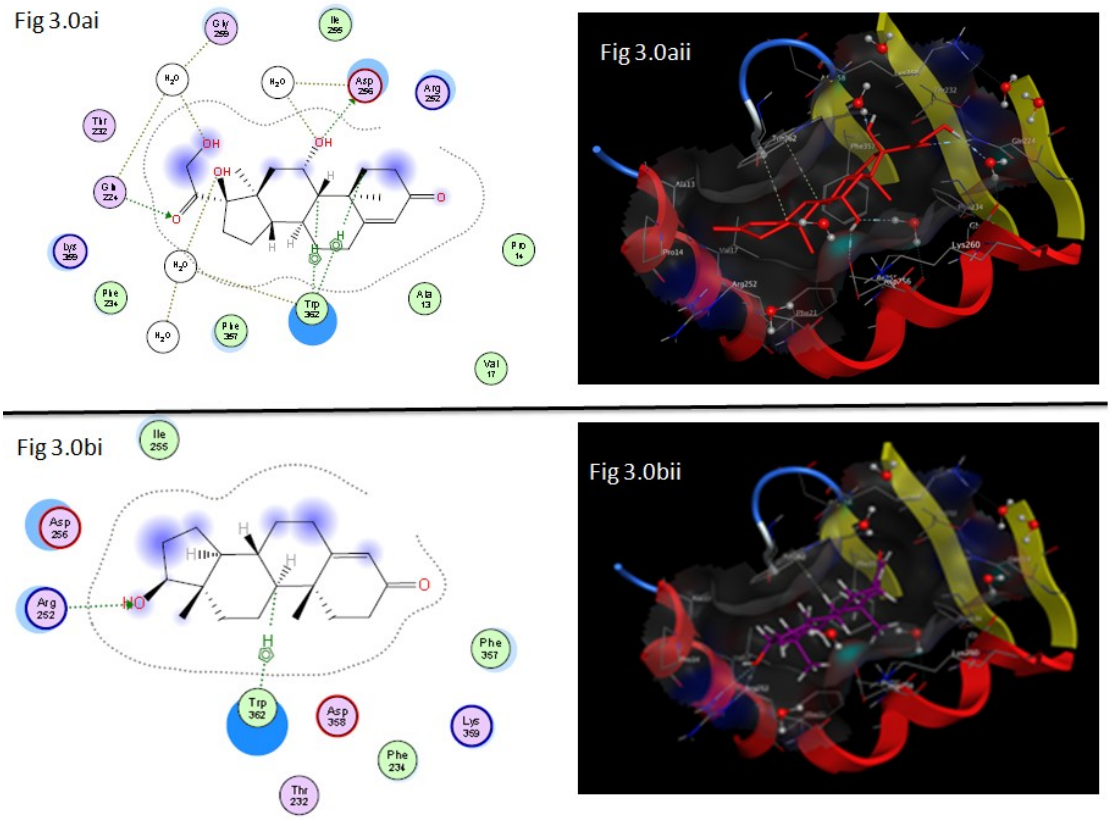

Figure 3.0a. Cortisol interaction with CBG i) 2D depiction, ii) surface and map depiction.

Figure 3.0b. Testosterone interaction with CBG i) 2D depiction, ii) surface and map depiction

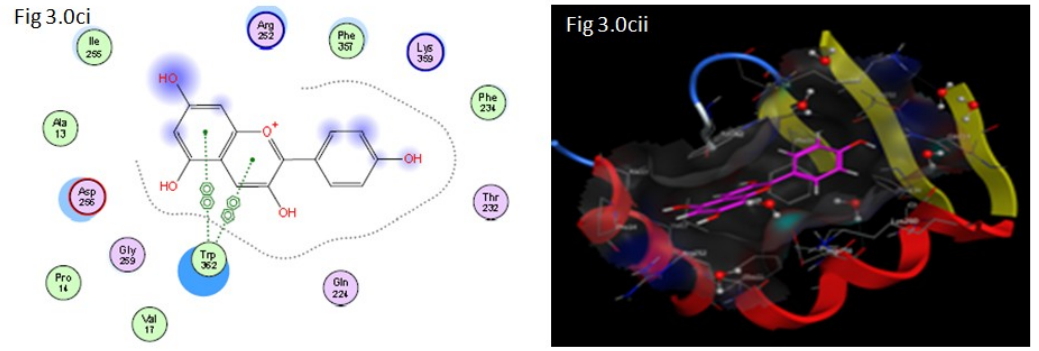

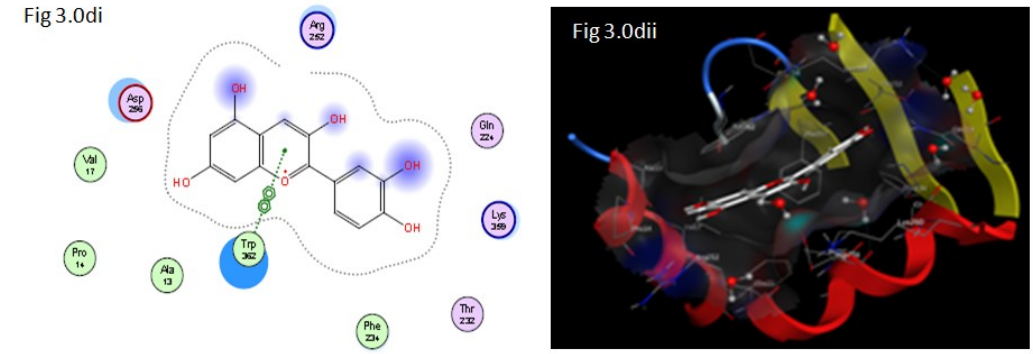

Figure 3.0c. Pelargonidin interaction with CBG i) 2D depiction, ii) surface and map depiction.

Figure 3.0d. Cyanidin interaction with CBG i) 2D depiction, ii) surface and map depiction.

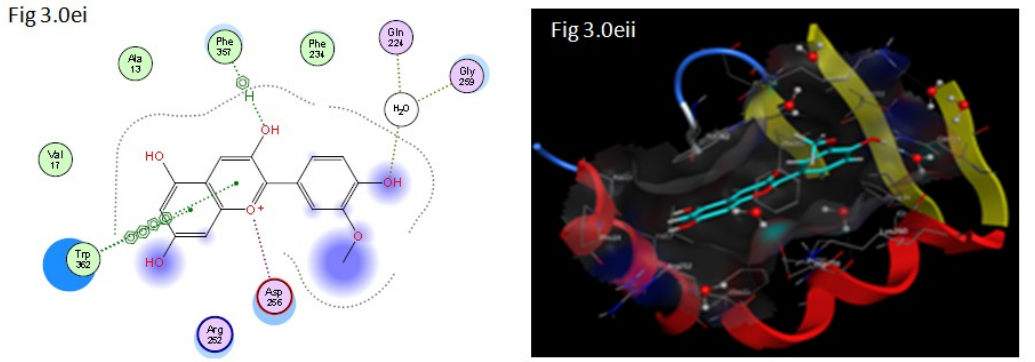

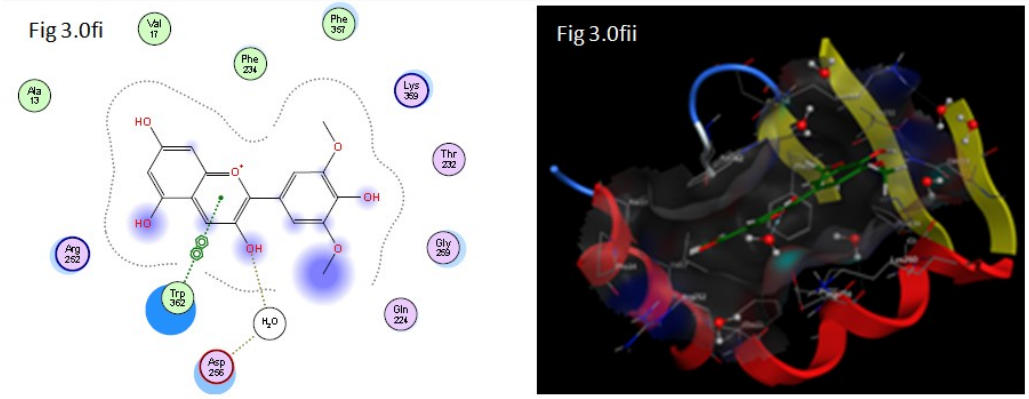

Figure 3.0e. Peonidin interaction with CBG i) 2D depiction, ii) surface and map depiction.

Figure 3.0f. Malvidin interaction with CBG i) 2D depiction, ii) surface and map depiction.

Table 1.0 Free energy of binding between CBG and Anthocyanidins and their glycone-derivatives

		GBVIWSA
1	cortisol	-8.2618
2	delphinidin-3- glucoside	-6.5539
3	estradiol	-6.5403
4	delphinidn	-6.4806
5	pelargonidin	-6.3221
6	malv-3-glucoside	-6.0742
7	peonidin	-6.0098
8	pelargonidin-3-glucoside	-5.9140
9	petunidin	-5.7971
10	petunidin-3-glucoside	-5.7855
11	cyanidin	-5.7728
12	peonidin-3-glucoside	-5.7702
13	malvidin	-5.6549
14	cyanidin-3-glucoside	-5.5748
15	testo.pdb	-3.0513